


2020

## **Binder Saturation, Layer Thickness, Drying Time and Their Effects on Dimensional Tolerance and Density of Cobalt Chrome - Tricalcium Phosphate Biocomposite**

John Ruprecht  
*Minnesota State University, Mankato*

Follow this and additional works at: <https://cornerstone.lib.mnsu.edu/etds>

 Part of the [Biomaterials Commons](#), [Biomechanical Engineering Commons](#), and the [Biomedical Devices and Instrumentation Commons](#)

---

### **Recommended Citation**

Ruprecht, J. (2020). Binder saturation, layer thickness, drying time and their effects on dimensional tolerance and density of cobalt chrome - tricalcium phosphate biocomposite [Master's thesis, Minnesota State University, Mankato]. Cornerstone: A Collection of Scholarly and Creative Works for Minnesota State University, Mankato. <https://cornerstone.lib.mnsu.edu/etds/1026>

This Thesis is brought to you for free and open access by the Graduate Theses, Dissertations, and Other Capstone Projects at Cornerstone: A Collection of Scholarly and Creative Works for Minnesota State University, Mankato. It has been accepted for inclusion in All Graduate Theses, Dissertations, and Other Capstone Projects by an authorized administrator of Cornerstone: A Collection of Scholarly and Creative Works for Minnesota State University, Mankato.

BINDER SATURATION, LAYER THICKNESS, DRYING TIME AND THEIR EFFECTS ON  
DIMENSIONAL TOLERANCE AND DENSITY OF COBALT CHROME - TRICALCIUM  
PHOSPHATE BIOCOMPOSITE

By

John Ruprecht

A thesis submitted in partial fulfillment of the requirements for the degree of Master of Science  
in Manufacturing Engineering Technology concentrating on Binder Jet 3D Printing at Minnesota  
State University, Mankato

Minnesota State University, Mankato, Minnesota, 56001, US

May 2020

4/17/2020

BINDER SATURATION, LAYER THICKNESS, DRYING TIME AND THEIR  
EFFECTS ON DIMENSIONAL TOLERANCE AND DENSITY OF COBALT  
CHROME - TRICALCIUM PHOSPHATE BIOCOMPOSITE

John Ruprecht

This thesis has been examined and approved by the following members of the student's  
committee.

---

Advisor

---

Committee Member

---

Committee Member

BINDER SATURATION, LAYER THICKNESS, DRYING TIME AND THEIR  
EFFECTS ON DIMENSIONAL TOLERANCE AND DENSITY OF COBALT  
CHROME - TRICALCIUM PHOSPHATE BIOCOMPOSITE

JOHN RUPRECHT

A THESIS SUBMITTED IN PARTIAL FULFILLMENT OF THE  
REQUIREMENTS FOR THE DEGREE OF  
MASTER OF SCIENCE IN MANUFACTURING ENGINEERING TECHNOLOGY

MINNESOTA STATE UNIVERSITY, MANKATO  
MANKATO, MINNESOTA  
MAY 2020

ABSTRACT

Traditional metals such as stainless steel, titanium and cobalt chrome are used in biomedical applications (implants, scaffolds, etc.) but suffer from issues such as osseointegration and compatibility with existing bone. One way to improve traditional biomaterials is to incorporate ceramics with these metals so that their mechanical properties can be similar to cortical bones. Tricalcium phosphate is such a ceramic with properties such that it can be used in the human body. This research explores the use of the Binder Jetting based additive manufacturing process to create a novel biocomposite made of cobalt chrome and tricalcium phosphate. Experiments were conducted and process parameters were varied to study their effect on the printing of this biocomposite. Layer thickness, binder saturation and drying time affected the dimensional tolerance and the density of the brown samples. This effect is important to understand so that the material can be optimized for use in specific applications

**TABLE OF CONTENTS**

|  |    |
|--|----|
| INTRODUCTION.....                            | 1  |
| BINDER JET-BASED ADDITIVE MANUFACTURING..... | 4  |
| PROCESS PARAMETERS.....                      | 5  |
| EXPERIMENTAL PLAN.....                       | 5  |
| RESULTS.....                                 | 7  |
| DISCUSSION.....                              | 11 |
| CONCLUSION.....                              | 12 |
| REFERENENCES.....                            | 14 |

## **Introduction**

A biomaterial is any material, natural or man-made, that can perform a bodily function or can replace a body part or tissue. Depending on their application, biomaterials can be made from polymers, metals, ceramics, or composites [1-3].

Biomedical implants can be classified into three major categories: external to the body (non-clinical, which includes surgical instruments, prosthetics, etc.), internal to the body and permanent (includes hip implants, knee implants, stents, etc.), and internal to the body & temporary (includes scaffolds, degradable screws and drug delivery systems) [1-3, 14].

According to FDA, a “permanently implantable device is a device that is intended to be placed into a surgically or naturally formed cavity of the human body for more than one year to continuously assist, restore, or replace the function of an organ system or structure of the human body throughout the useful life of the device.” Some examples include knee and hip implants. Temporary implants are commonly used in sports surgeries, such as in shoulder and knee ligamentous reconstruction and spinal reconstructive surgery [5, 6, 14].

The most common biomaterials for implants are metals, their alloys, ceramics, and polymers. In the past few years, cobalt alloys have gained popularity for being used as biomaterials for implants. Bones have elastic moduli 7–30 GPa, yield stress 30–70 MPa, compressive strength 100–230 MPa, and tensile strength 70–150 MPa. The first-generation implants focused on replacement of the bone with a metal implant. However, mechanical properties of metals differ considerably from natural bone (i.e. cobalt chrome alloys elastic modulus: 210 GPa, yield strength: 120–600 MPa, and tensile strength: 190–800 MPa) [3, 4, 7].

These differences lead to stress shielding resulting in loosening of the implant due to degradation of human tissues around implants and, consequently, further surgeries to replace the implants. Ceramics are inorganic materials with high compressive strength and biological inertness that make them suitable for scaffolds used in strengthening or replacing damaged bones and tissues. The most commonly used bioceramics are metallic oxides (e.g.  $\text{Al}_2\text{O}_3$ ,  $\text{MgO}$ ), calcium phosphate (e.g. hydroxyapatite (HA), tricalcium phosphate (TCP), octacalcium phosphate (OCP)), and glass ceramics (e.g. Bioglass, Ceravital).

Calcium phosphates have the best biocompatibility and properties closest to natural bones: elastic modulus 7–13 GPa, compressive strength 350–450 MPa, tensile strength 38–48 MPa, and flexural strength 100–120 MPa. However, they have poor fracture toughness and tensile strength that limits their application for bioimplants. Several in vitro and in vivo works have shown that calcium phosphates support the adhesion, differentiation, and proliferation of osseogenesis-related cells (e.g. osteoblasts, mesenchymal stem cells), and induce gene expression in bone cells. The most important calcium phosphate is hydroxyapatite (HA,  $\text{Ca}_{10}(\text{PO}_4)_6(\text{OH})_2$ ). With chemical characteristics similar to hard tissues such as bone and teeth, they promote hard tissue in growth and osseointegration when implanted into the human body. The porous structure of this material can be tailored to suit the interfacial surfaces of the implant. As a bulk material, HA lacks sufficient tensile strength and is too brittle to be used in most load bearing applications. In such cases, HA is coated onto a metal core or incorporated into polymers as composites. The ceramic coating on the titanium implants improves the surface bioactivity but often fails as a result of poor ceramic/metal interface bonding [8-11].

$\alpha$ -TCP and  $\beta$ -TCP are the two crystalline varieties of HA of interest in biological applications.  $\beta$ -TCP is the thermodynamically stable form at low temperature. It transforms into  $\alpha$ -TCP in the temperature range 1120–1170 °C.  $\beta$ -TCP is generally preferred in sintered ceramic implants, while  $\alpha$ -TCP is more commonly used in bone graft cements because of its hydrolysis properties. The requirements that allow bone ingrowth are a porosity of 30–70 vol%, a pore diameter between 300 and 800  $\mu\text{m}$ , and mechanical properties of 0.5–15 MPa. These being similar to cancellous bone.

Thus, there is a drive in the biomedical industry to create novel materials that behave very similar to bone and can be used for multiple applications from permanent to temporary implants. Furthermore, these materials need to be manufactured in a manner that would create porosity in situ for biological applications.

Due to the versatility of additive manufacturing, it is gaining a lot of popularity in the field of bone implants. Selective Laser Sintering, Selective Laser Melting, Electron Beam Melting and Binder jet manufacturing have all been used to create various porous structures for biomedical implants [7, 9]. To accomplish the various requirements of the implants it is necessary to create biocomposites that can have the strength properties of metals as well as the biological properties of bioceramics.

This research explores the use of the Binder Jet based additive manufacturing process to create a novel biocomposite made of cobalt chrome (CC) and tricalcium phosphate (TCP). Experiments were conducted and processing parameters were varied to study their effect on the printing of this biocomposite. Layer thickness, binder saturation, and drying time affected the dimensional tolerance and the density of the brown samples. This effect is important to understand so that the material can be optimized for use in specific applications.

### **Binder Jet-based Additive Manufacturing**

Binder Jetting additive manufacturing (AM) is a Drop on Demand (DoD) inkjet printing process in which binder is emitted through a nozzle to form a short jet. This jet condenses into a drop and the position at which each drop lands on substrate is controlled by relative motion between drop and the substrate. The nozzle head is piezoelectric and uses the deformation of ceramic element to generate a pressure pulse needed to eject the binder. Typical drop diameters vary from 10–100  $\mu\text{m}$ , drop volumes vary from 0.5–500 pl, and the drop speeds are 5–8 m/s [15].

The main technique of manufacture using the Binder Jet process is as follows: (a) The CAD model is converted to an STL file and a slicer is used to slice it into layers, (b) Each layer begins with a thin distribution of powder spread over the surface of a powder bed, (c) Using a technology similar to ink-jet printing, a binder material selectively joins particles where the object is to be formed, (d) A piston that supports the powder bed and the part-in-progress lowers so that the next powder layer can be spread and selectively joined, (e) This layer-by-layer process repeats until the part is completed, (f) Following a heat treatment, unbound powder is removed and the metal powder is sintered together. Fig. 1 shows the details of the whole process.

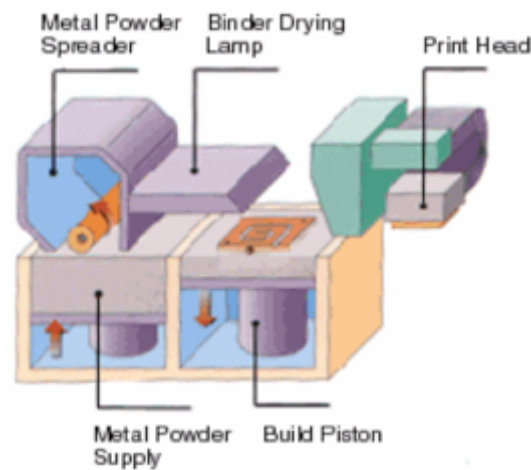


*Fig. 1: Schematic of the Binder Jet Process (Courtesy The ExOne Company)*

### **Process parameters**

The Binder Jet process described above can be divided into 3 basic steps: 1) Binding 2) Curing and 3) Sintering. There are various process parameters that can be changed to obtain a customized part in each of these steps. These include powder size, layer thickness during binding, part orientation in bed, heater power, roller speed, curing temperature, curing time, sintering time, sintering temperature, and sintering atmosphere. In this research we concentrated on the feasibility of printing of the CC and TCP biocomposite.

### **Experimental Plan**

The materials used in the study were cobalt chrome (Co 212-H, Sandvik Osprey), which has a mean particle size of 53  $\mu\text{m}$  and an apparent density of 3.15 g/cc. The chemical composition of Co 212-H is shown in Table 1.

*Table 1: Chemical composition of Co 212-H (wt %)*

| C        | Ni       | Fe       | Si       | Mn       | Mo      | Cr        | Co      |
|----------|----------|----------|----------|----------|---------|-----------|---------|
| 0.02 max | 0.10 max | 0.75 max | 1.00 max | 1.00 max | 5.0–7.0 | 27.0–30.0 | Balance |

$\beta$ -Tricalcium Phosphate (TCP) was obtained from Sigma-Aldrich (21218) with a mean particle size of 5  $\mu\text{m}$  and an apparent density of 1.92 g/cc. Scanning Electron Microscope (JEOL JSM-6510MV) was used to look at the sizes and distribution of the powders before the process. The images are shown in Fig. 2.

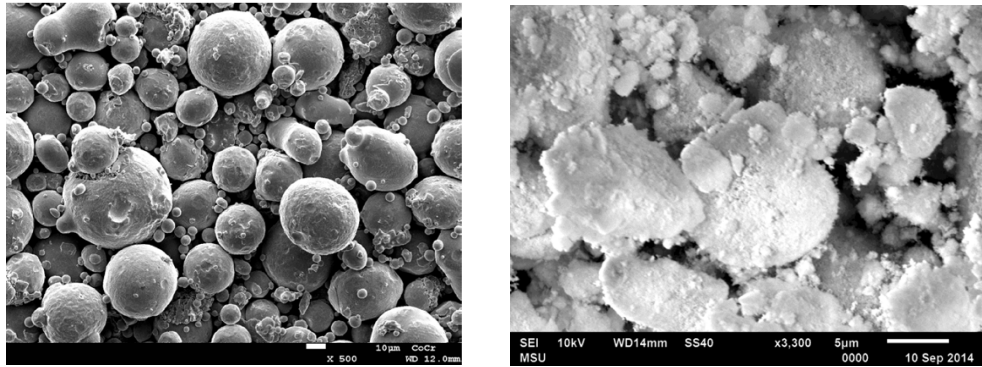


*Fig. 2: SEM Micrographs for Co 212-H and TCP*

Co 212-H was used as a benchmark and is called Sample Set 1. The two powders were mixed in with 80% Co 212-H -20% TCP volume fraction and this is called sample set 2.

The 2 sample sets were then used as the input powders in the Binder Jet additive manufacturing. To understand the effect of printing parameters of the Binder Jet process on the print quality, multiple factors and levels were chosen based on prior experience (Table 2). After the printing, all the samples were cured at 175 °C for 3 hours.

The print quality was measured by two means: dimensional tolerance compared to the CAD model and the density of the part after the printing. Two different size of parts were printed to study the effect of size on the dimensional tolerance. The CAD drawings of the parts with nominal dimensions is shown in Fig. 3. Eight parts of 10 mm and three parts of 30 mm were printed for the corresponding experimental run.

*Table 2: Factors and levels for Design of experiments*

| S.No. | Factor                                    | Levels  |
|-------|---|---------|
| 1     | Layer Thickness ( $\mu\text{m}$ )         | 60, 90  |
| 2     | Binder Saturation (as % of printhead max) | 80, 100 |
| 3     | Drying Time between layers (sec)          | 15, 20  |
| 4     | Sample Size (Outside dimension in mm)     | 10, 30  |

If a full factorial experimental design would be done on these parameters, it would require a total of 16 experiments. Instead a half factorial experimental design was chosen and 8 experiments were conducted. The experimental design matrix is shown in Table 3.

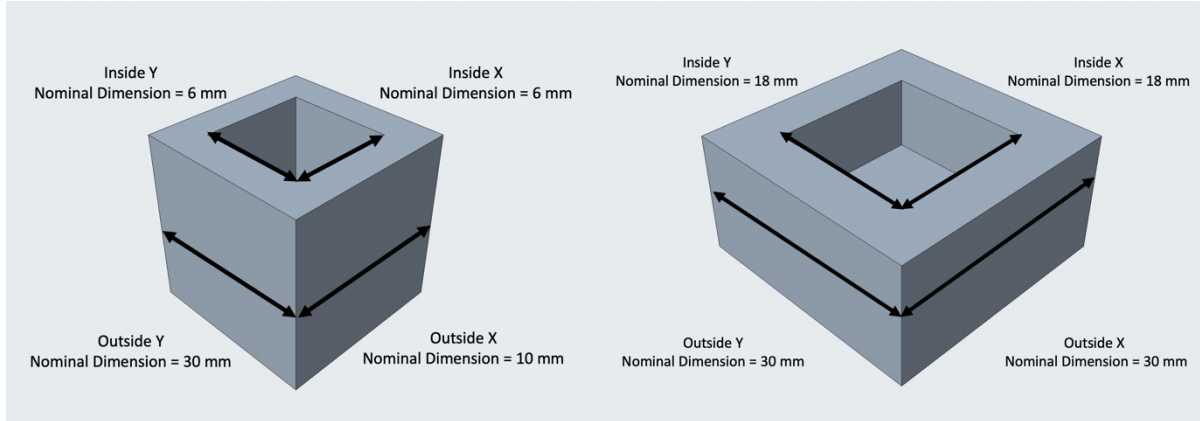


*Fig. 3: CAD models with dimensions for 10 mm and 30 mm samples*

*Table 3: Experimental design matrix*

| Experiment No. | Layer Thickness<br>( $\mu\text{m}$ ) | Binder Saturation<br>(%) | Drying Time<br>(sec) | Sample Size<br>(mm) |
|----------------|--------------------------------------|--------------------------|----------------------|---------------------|
| 1              | 90                                   | 100                      | 15                   | 10                  |
| 2              | 60                                   | 100                      | 20                   | 10                  |
| 3              | 90                                   | 100                      | 20                   | 30                  |
| 4              | 90                                   | 80                       | 20                   | 10                  |
| 5              | 60                                   | 80                       | 15                   | 10                  |
| 6              | 90                                   | 80                       | 15                   | 30                  |
| 7              | 60                                   | 100                      | 15                   | 30                  |
| 8              | 60                                   | 80                       | 20                   | 30                  |

## **Results**

After the parts were printed, they were weighed and measured for the outside  $X$ , outside  $Y$ , inside  $X$  and inside  $Y$  dimensions. Dimensional deviation from the CAD model was calculated according to the following formula for each of the four dimensions:

$$\text{Dimensional Deviation (\%)} = \frac{\text{Nominal Dimension (CAD)} - \text{Measured Dimension}}{\text{Nominal Dimension (CAD)}} * 100\%$$

The box plots for the two different sample sets and their dimensional variations are shown in Fig. 4–6.

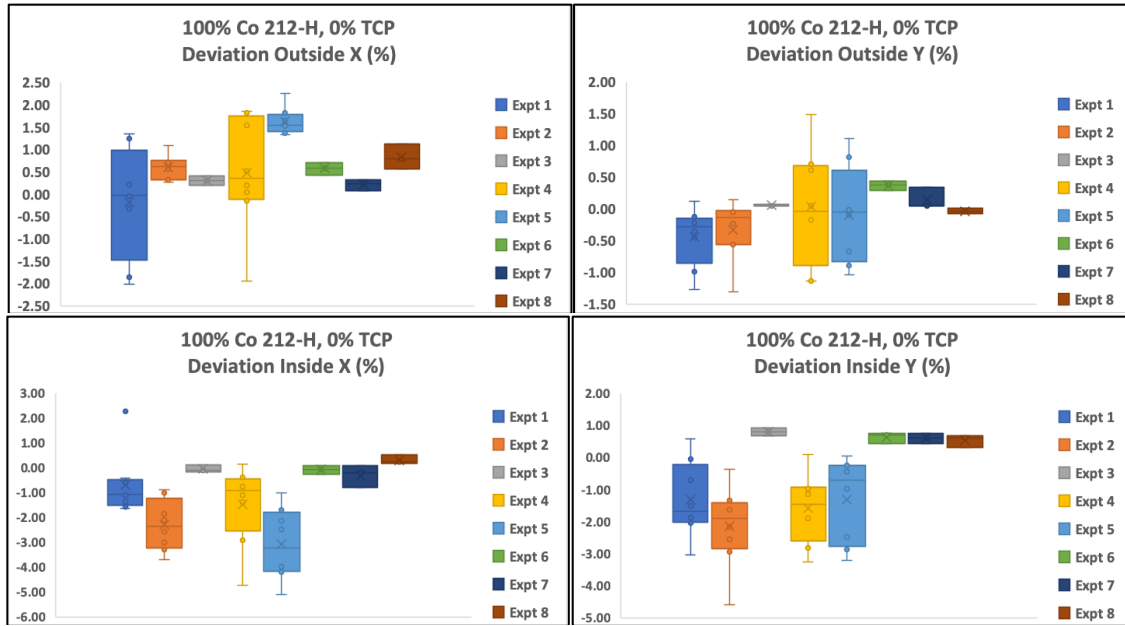


Fig. 4: Dimensional variation along two directions for sample set 1 (100% Co 212-H, 0% TCP)

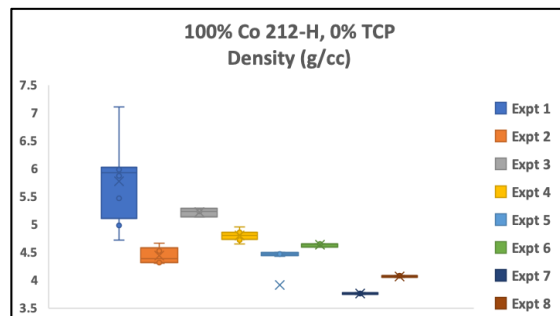


Fig. 5: Density variation for sample set 1 (100% Co 212-H, 0% TCP)

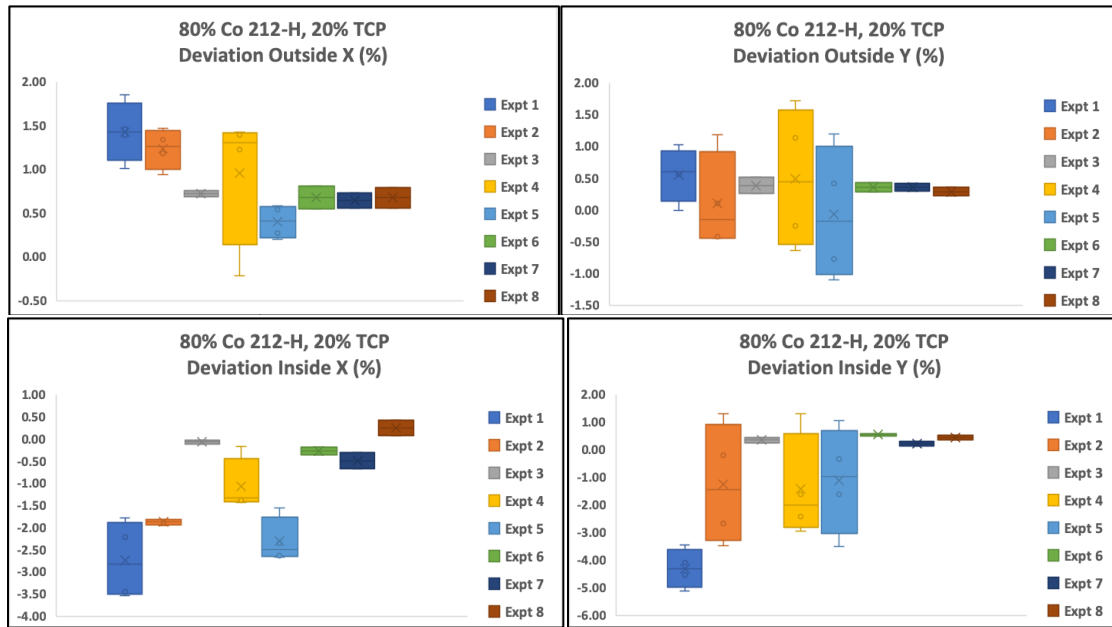


Fig. 6: Dimensional variation along 2 directions for sample set 2 (80% Co 212-H, 20% TCP)

The samples from various experiments were also photographed to look at the printing errors such as bleed out, distorted walls, rough surface, excess material etc. These are shown in Fig. 7–8.

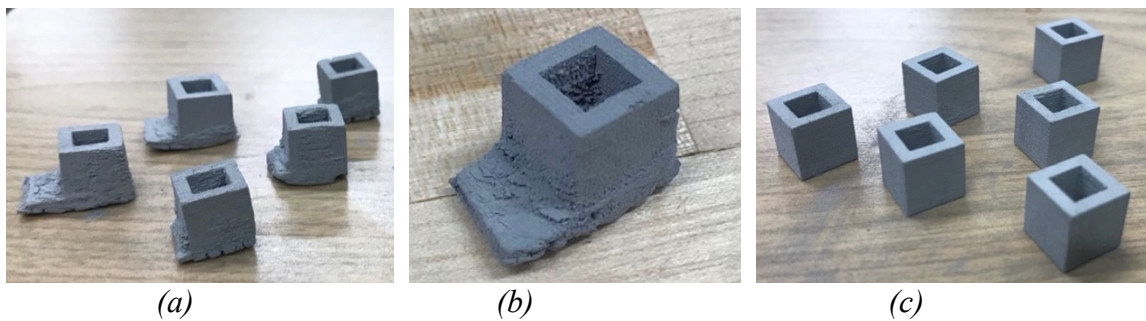


Fig. 7: (a) 10 mm samples with printing bleed out, (b) 10 mm sample with printing error (c) Good 10 mm samples

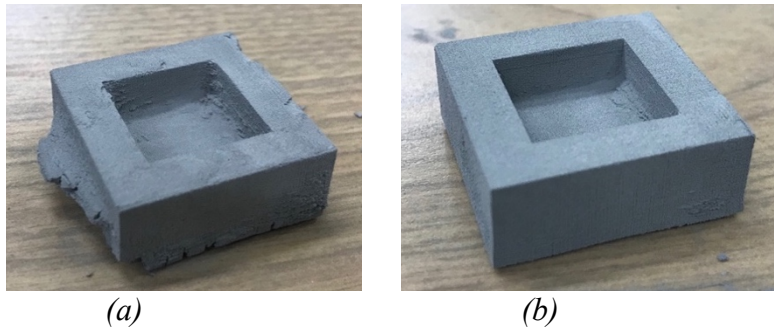


Fig. 8: (a) 30 mm sample depicting printing error (b) Good 30 mm sample

The response surface analysis of all the results was done using MINITAB. Only the main factors were considered in the analysis and the interaction between the factors was ignored for this study since the aim is to find the process parameters important for dimensional variations. A typical fitted response surface is shown in Fig. 9.

| 0% HA  |        |            |             |           |         |
|--|--------|------------|-------------|-----------|---------|
| Response Surface Regression: Outside X versus LT, BS, DT, SS |        |            |             |           |         |
| Analysis of Variance   |        |            |             |           |         |
| Source   | DF     | Adj SS     | Adj MS      | F-Value   | P-Value |
| Model  | 7      | 3519.03    | 502.72      | 70719.03  | 0.000   |
| Linear   | 4      | 3518.97    | 879.74      | 123756.20 | 0.000   |
| LT   | 1      | 0.03       | 0.03        | 4.39      | 0.043   |
| BS   | 1      | 0.10       | 0.10        | 14.67     | 0.000   |
| DT   | 1      | 0.00       | 0.00        | 0.34      | 0.566   |
| SS   | 1      | 3518.83    | 3518.83     | 495005.41 | 0.000   |
| Error  | 36     | 0.26       | 0.01        |           |         |
| Total  | 43     | 3519.28    |             |           |         |
| Model Summary  |        |            |             |           |         |
| S  | R-sq   | R-sq (adj) | R-sq (pred) |           |         |
| 0.0843129  | 99.99% | 99.99%     | 99.99%      |           |         |

Fig. 9: Response surface result from MINITAB. LT: Layer Thickness, BS: Binder Saturation, DT: Drying time and SS: Sample Size

All the response surfaces were analyzed and the results of the P-values were summarized to identify the significant factors in each case. The summary of P-values is shown in Table 4 and 5.

*Table 4: P-Values for 100% Co 212-H, 0% TCP Samples*

|                  | <b>Layer Thickness</b> | <b>Binder Saturation</b> | <b>Drying time</b> | <b>Sample Size</b> |
|------------------|------------------------|--------------------------|--------------------|--------------------|
| <b>Outside X</b> | 0.043                  | 0.001                    | 0.566              | 0.001              |
| <b>Inside X</b>  | 0.107                  | 0.901                    | 0.250              | 0.001              |
| <b>Outside Y</b> | 0.056                  | 0.092                    | 0.149              | 0.001              |
| <b>Inside Y</b>  | 0.140                  | 0.932                    | 0.585              | 0.001              |
| <b>Density</b>   | 0.001                  | 0.013                    | 0.814              | 0.001              |

*Table 5: P-Values for 80% Co 212-H, 20% TCP Samples*

|                  | <b>Layer Thickness</b> | <b>Binder Saturation</b> | <b>Drying time</b> | <b>Sample Size</b> |
|------------------|------------------------|--------------------------|--------------------|--------------------|
| <b>Outside X</b> | 0.012                  | 0.103                    | 0.060              | 0.001              |
| <b>Inside X</b>  | 0.112                  | 0.012                    | 0.001              | 0.001              |
| <b>Outside Y</b> | 0.066                  | 0.099                    | 0.093              | 0.001              |
| <b>Inside Y</b>  | 0.136                  | 0.131                    | 0.013              | 0.001              |
| <b>Density</b>   | 0.001                  | 0.089                    | 0.234              | 0.001              |

### **Discussion**

The study of various printing parameters and their effect on dimensions, surface finish, and density of a novel biocomposite are studied in this work. Results from the various tests, the box plots and the response surface analysis show the following:

- a) There is a difference in the dimensional variations and density for both the 0% and 20% TCP samples.
- b) Layer thickness and sample sizes are significant factors in both the sample sets. Thus, the dimension of the part, its surface and density are significantly affected by the layer thickness of the Binder Jet process. This is expected because the layer thickness affects the compaction of each layer and hence determines how much binder can saturate each powder layer.

- c) Drying time is not a significant factor in 0% TCP samples but is important for the 20% TCP samples. The TCP is a much softer material than Co 212-H and hence the binder saturates the powder a lot more in this case. This can result in material bleed outs or layers being dragged on another layer if it has not dried enough.
- d) Similarly, binder saturation affects the dimensional accuracy more in case of 20% TCP samples than in the case of 0% TCP samples. In fact, in 0% TCP samples, binder saturation does not affect the inside dimensions. This is because once a layer is formed, the outside surface is more prone to the distortion or dislocation than the inside surface.
- e) The 30 mm samples have much smaller variation in dimensions than the 10 mm samples. This might be because the larger surface area is more uniformly spread and dried than the smaller surface area of 10 mm samples.
- f) By looking at the samples visually and their dimensions, Experiment 5 (60  $\mu$ m Layer thickness, 80% binder saturation and 15 sec drying time) performed the best for 0% TCP Samples, 10 mm size. In case of 20% TCP samples, Experiment 4 (80  $\mu$ m Layer thickness, 80% binder saturation and 20 sec drying time) performed the best.
- g) There is a wide variation in the density of green parts depending upon the process parameters. This property can be exploited to control the porosity of the parts made by various materials.

### **Conclusions**

Traditional metals such as stainless steel, titanium and cobalt chrome are used in biomedical applications (implants, scaffolds, etc.) but suffer from issues such as osseointegration and compatibility with existing bone. One way to improve traditional biomaterials is to incorporate

ceramics with these metals so that their mechanical properties can be similar to cortical bones. TCP is such a ceramic with properties that it can be used in human body. This research explores the use of the Binder Jet based additive manufacturing process to create a novel biocomposite made of cobalt chrome and tricalcium phosphate. Experiments were conducted and processing parameters were varied to study their effect on the printing of this biocomposite.

It is found that layer thickness is significant factor for printing with 0% TCP and 20% TCP samples. However, drying time is only significant for 20% TCP samples because of the soft nature of TCP powder and a similar effect is found with binder saturation. Thus, printing parameters are crucial in manufacturing parts from Binder Jet additive manufacturing.

Further research needs to be conducted to take the best printing parameters, use the samples from this configuration, and study the effect of sintering parameters on the strength and biocompatibility of these samples.

### **References**

1. Tarafder, S., 2013. Physicomechanical, In Vitro and in Vivo Performance of 3D Printed Doped Tricalcium Phosphate Scaffolds for Bone Tissue Engineering and Drug Delivery, Ph.D. *Dissertation*,
2. Butscher, A., Böhner, M., Hofmann, S., Gauckler, L., Müller, R., 2011, Structural and material approaches to bone tissue engineering in powder-based three-dimensional printing, *Acta Biomaterialia* 7, pp. 907–920.
3. Ahmadi, S. M., Yavari, S.A., Wauthle, R., Pouran, B., Schrooten, J., Weinans H., Zadpoor, A.A., 2015. Additively Manufactured Open-Cell Porous Biomaterials Made from Six Different Space-Filling Unit Cells: The Mechanical and Morphological Properties, *Materials*, 8, pp. 1871-1896; doi:10.3390/ma8041871.
4. Kolan, K., Thomas, A., Leu, M.C., Hilmas, G., 2015. In vitro assessment of laser sintered bioactive glass scaffolds with different pore geometries, *Rapid Prototyping Journal*, Vol. 21 Iss: 2, pp.152 – 158.
5. Bose, S., Vahabzadeh, S., Bandyopadhyay, A., 2013. Bone tissue engineering using 3D printing, *Materials today*, Volume 16, Issue 12, pp. 496–504.
6. Bose, S., Roy, M., Bandyopadhyay, A., 2012. Recent advances in bone tissue engineering scaffolds, *Trends in Biotechnology*, Volume 30, Issue 10, pp. 546–554.
7. Alvarez, K., Nakajima, H., 2009. Metallic Scaffolds for Bone Regeneration, *Materials*, 2, pp. 790-832; doi:10.3390/ma2030790.

8. MitraAsadi-Eydivand, MehranSolati-Hashjin, Farzad, A., 2016. Effect of technical parameters on porous structure and strength of 3D printed calcium sulfate prototypes, *Robotics and Computer-Integrated Manufacturing*, 37, pp. 57–67.
9. Cox, S.C., Thornby, J.A, Gibbons, G.J., Williams, M.A, Mallick, K.K, 2015. 3D printing of porous hydroxyapatite scaffolds intended for use in bone tissue engineering applications, *Materials Science and Engineering C* 47, pp. 237–247.
10. Ratner, B., Hoffman, A., Schoen, F., Lemons, J., 2012. Biomaterials Science : An introduction to materials in medicine, Academic Press, MA.
11. Lou, T., Wang, X., Song, G., Gu, Z., Yang, Z., 2015. Structure and properties of PLLA/b-TCP nanocomposite scaffolds for bone tissue engineering, *J Mater Sci: Mater Med*, pp. 26-34.
12. Ashby, M.F, Evans, A.G., Fleck, N.A., Gibson, N.A., Hutchinson, J.W., Wadley, H.N.G., 2000. Metal Foams: A Design Guide, *Butterworth-Heinemann*
13. German, R., 1996. Sintering Theory and Practice, *Wiley-VCH*
14. Bartolo, P., Kruth, J., Silva, J., Levy, G., Malshe, A., Rajurkar, K., Mitsuishi, M., Ciurana, J., Leu, M., “Biomedical production of implants by additive electro-chemical and physical processes”, *CIRP Annals - Manufacturing Technology* 61 (2012), 635-655
15. Hoath, S., 2016. “Fundamentals of Inkjet Printing: The science of inkjets and droplets”, Wiley-VCH Verlag GmbH & Co.